

Investigating Detect-and-Avoid Surveillance Performance for Unmanned Aircraft Systems

Chunki Park* and Seung Man Lee†

UC Santa Cruz, NASA Ames Research Center, Moffett Field, CA 94035, USA

Eric R. Mueller‡

NASA Ames Research Center, Moffett Field, CA 94035, USA

Most unmanned aircraft systems will be required to be equipped with a detect-and-avoid system that is capable of maintaining appropriate separation from other aircraft to operate in the National Airspace System. A surveillance system is one of the critical components of detect-and-avoid systems in order to predict potential conflicts with adequate lead time to remain “well clear” of other aircraft. The performance requirements of surveillance systems to detect and track intruder aircraft will depend on the encounter geometries that unmanned aircraft are expected to have with other aircraft in the airspace. In this study, a database of unmitigated encounters between unmanned aircraft and conventional manned aircraft operating under visual flight rules is created without maneuvering any aircraft to mitigate the risk of a separation violation. The encounter database is built through fast-time simulation of a large number of unmanned aircraft conducting various missions in the presence of historical visual flight rules traffic as recorded from live airspace operations. Analysis of the resulting encounter geometries suggests how the overall safety and performance of a surveillance system may relate to surveillance parameters such as surveillance range, horizontal and vertical fields of regard. This paper proposed and investigated potential safety and performance metrics for evaluating the performance of a surveillance system, such as the ratio of undetected and late-detected separation violations, and the time to violation at first detection for given sets of surveillance parameters. These example metrics demonstrate the utility of the database of encounters created in this work. It is expected that this database will be useful in the derivation of surveillance system requirements for detect-and-avoid systems.

Nomenclature

<i>DMOD</i>	Distance Modifier
<i>HMD</i>	Horizontal Miss Distance
<i>TCOA</i>	Time Threshold for Time to Co-Altitude
<i>TTHR</i>	Time Threshold for Modified Tau
<i>ZTHR</i>	Altitude Threshold
DAA	Detect and Avoid
hFOR	Horizontal Field of Regard
vFOR	Vertical Field of Regard
WCV	Well Clear Violation

*Assistant Research Scientist, Aviation Systems Division, M/S 210-8, Member AIAA, chunki.park@nasa.gov

†Associate Research Scientist, Aviation Systems Division, M/S 210-8, Senior Member AIAA, seungman.lee@nasa.gov

‡Aerospace Engineer, Aviation Systems Division, M/S 210-10, Associate Fellow AIAA, eric.mueller@nasa.gov

I. Introduction

The demand to fly unmanned aircraft systems (UAS) in the National Airspace System (NAS) for a wide variety of civil, public and federal purposes is driving research into concepts and technologies that allow UAS to comply with existing operational requirements. A vital requirement codified in Title 14 CFR Part 91.113 is that pilots “see and avoid other aircraft.” In order to comply with this regulation without the presence of an onboard pilot, UAS must employ technologies that allow it to carry out this capability.^{1,2} Technologies typically used to avoid other aircraft are surveillance sensors, threat detection and resolution algorithms, and a display that allows pilot interaction with the algorithms; together these are referred to as the detect-and-avoid (DAA) system. The significant difference between the task of avoiding aircraft by looking for them out of the aircraft windscreen and avoiding symbols on a display means the human visual system cannot be used to derive requirements for the surveillance sensors. Instead, the sensor requirements must be derived from a UAS ability to avoid aircraft as a function of those surveillance requirements, which in combination with other DAA requirements and NAS characteristics would allow the UAS to meet a given level of safety. The efficacy of the avoidance function is sensitive to the characteristics of encounters the UAS is expected to have with other aircraft, and so the surveillance requirements must be based in part on the encounter characteristics. The encounters UAS are likely to have with other aircraft in a future NAS are not well understood, particularly given the uncertainty in the composition of the UAS fleet’s aerodynamic performance and mission types.

The surveillance requirements, in combination with other DAA characteristics, are selected to achieve a level of safety. This level of safety is, broadly speaking, dependent upon two important variables: the rate at which a UAS encounters other aircraft and the effectiveness of the DAA system in mitigating those encounters.¹ The expected rate of near mid-air collisions (NMACs) was calculated for a single UAS track repeated across time and space and flown against real aircraft tracks; a rate of approximately 3 NMACs per 10,000 UAS flight hours was estimated.³ To evaluate the second variable relating to system safety, a larger set of aircraft tracks was processed into an encounter model,⁴ and the resulting sets of encounters were used to derive a risk-based threshold for the airborne separation standard the DAA system is expected to maintain (i.e. “well-clear”).⁵ This effort informed encounter characteristics between two Visual Flight Rules (VFR) aircraft, but its goal was not to specify the distributions of encounters a DAA surveillance system would be required to detect. In addition, the encounter model was based on existing VFR aircraft operations and so does not include the aerodynamic characteristics or mission profiles that UAS are likely to fly. Further, the FAA has indicated that UAS should be flying according to Instrument Flight Rules (IFR),² which will create a different set of encounters than would be expected between two aircraft operating VFR. Surveillance system requirements should be based on the encounters between IFR UAS and VFR manned aircraft. A recent study evaluated the encounter rates and some encounter characteristics between IFR UAS and other IFR aircraft and incorporated new aerodynamic performance and mission characteristics.⁶ The distribution of encounter characteristics between UAS operating IFR and manned aircraft operating VFR, and the relationship of those encounters to typical surveillance system characteristics like detection range and field of regard (FOR) is currently unknown.

This research characterizes encounters between IFR UAS and VFR manned aircraft in terms of the surveillance system requirements that will eventually be levied on DAA systems. The results are compiled from the simulation of tens of thousands of UAS flight hours comprising hundreds of different flight plans against tens of thousands of VFR aircraft. The encounter statistics indicate times to well-clear violation at which aircraft are detected given a set of surveillance characteristics. This information will allow selection of a minimum surveillance range and FOR requirement in order to detect a given percentage of intruding aircraft. An upper bound on the surveillance range requirement can also be established by this research as a function of the time at which a threat aircraft must be declared to the pilot. Finally, the rates of undetected and late-detected encounters as a function of surveillance range and FOR are provided. Together, these encounter statistics’ sensitivities to surveillance system parameters enable the UAS designer to do trade studies in pursuit of an optimal configuration of the DAA system for their application.

The rest of the paper is organized as follows: Section II introduces a generic sensor model for DAA systems and the main surveillance parameters. Section III describes the experimental setup for the air traffic simulation and methodologies for analyzing the simulation results. Results are presented in Section IV and V. Section VI provides conclusions and discusses the directions for future research.

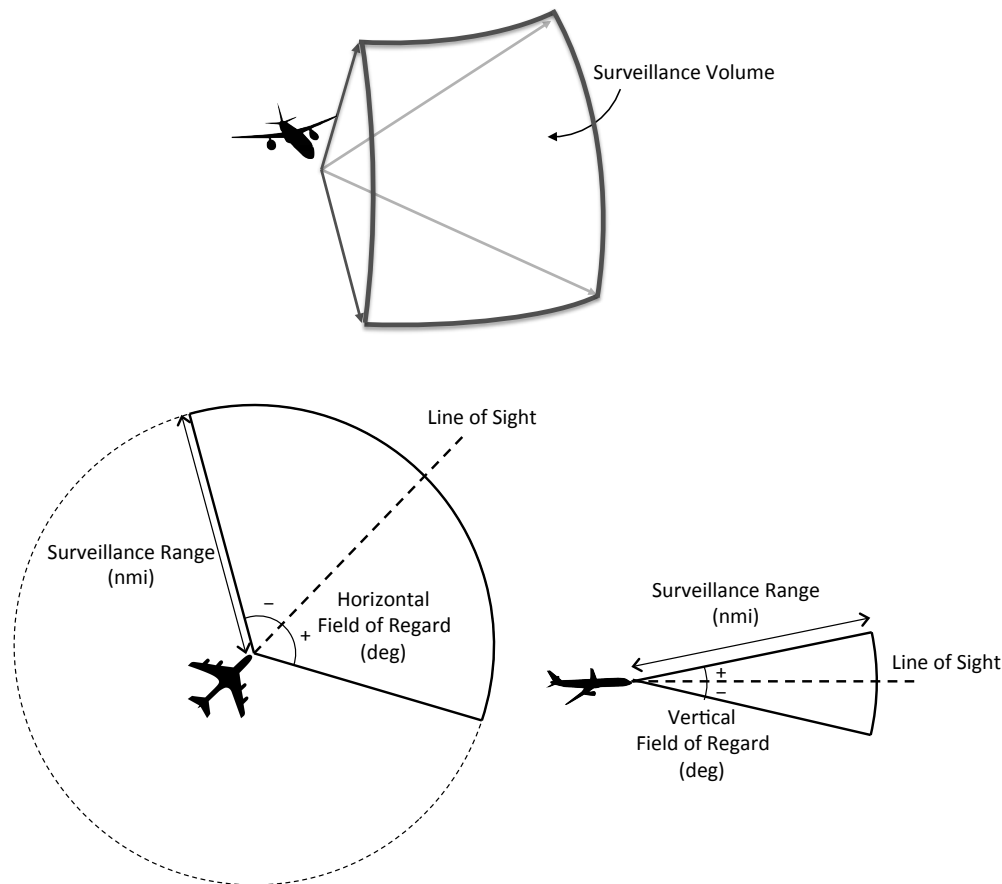


Figure 1. A generic sensor model that is represented by the surveillance range and fields of regard. The figure on the top shows the 3D shape of the surveillance volume: the two figures on the bottom illustrate the range and field of regard. In addition to these two main surveillance parameters, the sensor scan (information update) is another sensor parameter.

II. Brief Introduction to a Generic Sensor Model for DAA Systems

A UAS flight is required to have the capability corresponding to the on-board human pilot's "see" function. Therefore, the UAS needs to be equipped with sensor systems that can detect the collision and conflict risks posed by other aircraft. Although there are some cooperative technologies for safe traffic separation such as traffic alert and collision avoidance system (TCAS), automatic dependent surveillance-broadcast (ADS-B), and airborne collision avoidance system (ACAS), not every aircraft flying in the NAS possesses these cooperative sensors. An alternative means must be employed to detect such aircraft.

Contrary to cooperative systems, noncooperative systems do not rely on other aircraft equipped with cooperative systems. The noncooperative systems detect obstacles for themselves, and thus they can detect general aviation (GA) flights that do not have cooperative systems and also detect ground-based obstacles such as transmitting towers, mountain peaks, and power lines. This paper focuses on GA flight detection. The noncooperative systems are categorized into two systems. One is an active system, such as a radar or laser, which actively transmits signals to detect obstacles. The other is a passive system, such as electro-optical (EO), infrared (IR), and motion detection (MD) systems, which do not transmit signals but do detect naturally occurring energy, like IR or visible light waves, emitted from obstacles.⁷

As mentioned earlier, one objective of this study is exploring requirements for the surveillance systems equipped in UAS. The preliminary requirements include the minimum detection capability for the systems that mainly depends on the three technical characteristics of sensors: the surveillance range, field of regard, and the scan (information update) rate. Therefore, this study uses a generic sensor model that is represented by those three sensor characteristics. Figure 1 shows the generic sensor model.

III. Experimental Method

The performance requirements of surveillance systems to detect and track intruder aircraft will depend on the encounter geometries that unmanned aircraft are expected to have with other aircraft in the airspace. Thus, in this study, unmitigated encounters between UAS and VFR flights without maneuvering any aircraft to mitigate the risk of a well-clear violation were investigated through a fast-time simulation of a large number of unmanned aircraft conducting various missions in the presence of historical VFR flights on a single day. Analysis of the resulting encounter geometries suggests how the overall safety and performance of a surveillance system are related to the surveillance sensor parameters such as surveillance range, horizontal and vertical fields of regard.

A. Definition of “well-clear violation”

As mentioned in the introductory section, manned aircraft have the ability to “see and avoid” other aircraft, as required by regulations governing the general operation of aircraft in the NAS under Title 14 CFR Part 91, Parts 91.111 (Operating near other aircraft) and 91.113 (Right of Way Rules: Except water operations). These and other regulations state that aircraft must remain “well-clear” of other aircraft and avoid collisions. The DAA system of UAS is expected to provide a means to replace an onboard pilots’ ability to see and avoid other traffic in a manner that preserves the safety level of the airspace and the efficiency of the air traffic system. Since remaining “well-clear” is a subjective matter determined by individual onboard pilots, a quantitative definition is required.

A well-clear violation generally occurs when two aircraft are projected to be within a certain horizontal and vertical distance from each other and the time to this loss of separation is below a particular time threshold. The definition has been actively discussed by the detect-and-avoid Science and Research Panel (SARP).¹ This paper uses the following proposed definition,⁸

$$R_{xy} \leq DMOD \quad \text{or} \quad (P_{cpa} \leq HMD \quad \text{and} \quad 0 \leq \tau_{mod} \leq TTHR)$$

and

$$R_z \leq ZTHR \quad \text{or} \quad (0 \leq T_{coa} \leq TCOA),$$

where R_{xy} : Horizontal range,
 P_{cpa} : Predicted horizontal range at time of closest point of approach,
 τ_{mod} : Modified tau $\begin{cases} -\frac{(R_{xy}^2 - DMOD^2)}{R_{xy}\dot{R}_{xy}} & : R_{xy} \geq DMOD \\ 0 & : R_{xy} < DMOD, \end{cases}$
 R_z : Relative altitude,
 T_{coa} : Time to co-altitude,

$$DMOD = 6000 \text{ ft},$$

$$HMD = 6000 \text{ ft},$$

$$ZTHR = 475 \text{ ft},$$

$$TTHR = 30 \text{ sec},$$

$$TCOA = 20 \text{ sec}.$$

To calculate P_{cpa} and T_{coa} , dead reckoning is used to predict aircraft’s future positions as in Ref.[8]. In the rest of this paper, two terms, “well-clear violation” and “encounter,” have the same meaning. In addition, the intruders that cause well-clear violations are referred to as “threats” to distinguish them from intruders that do not cause well-clear violations.

B. Analysis procedure

The performance of a generic surveillance system can be assessed in terms of its ability to detect well-clear violations. Thus, in this paper, the characteristics of well-clear violations between UAS flights and VFR

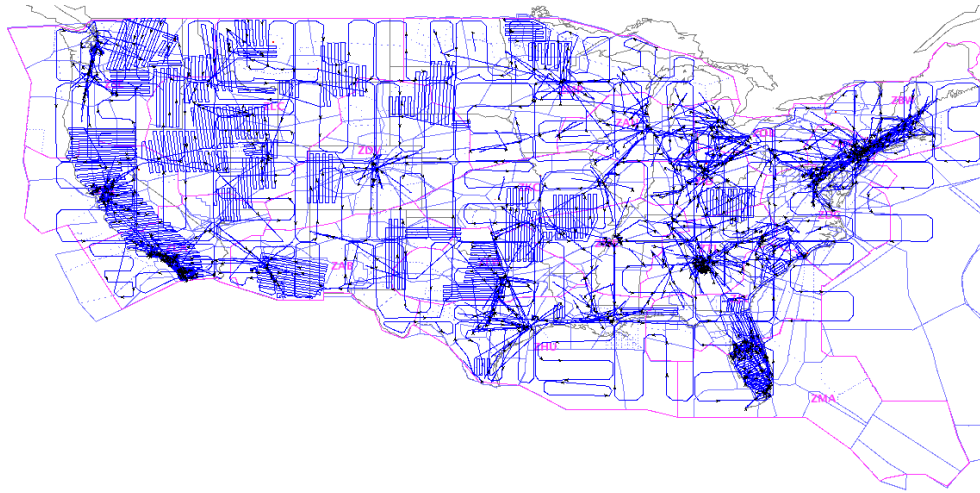


Figure 2. NAS-wide UAS mission profile, UAS tracks in blue

flights were first investigated independent of specific surveillance sensor parameters. The relative geometric positions of intruders at the point of a well-clear violation were measured. Also, their relative positions at different times prior to the violations were explored. The distances and horizontal/vertical angles to those intruders can give us clues to the required surveillance performance. Through this overall statistical analysis of well-clear violation geometric properties, the relationships between the violations and surveillance parameters were identified and the discrete values for each surveillance parameter were offered for detailed analysis on several specific surveillance volumes. In this study, the sensor scan rate is fixed to 2 seconds.

Next, based on the overall analysis, sets of surveillance parameters were selected and the surveillance performance was investigated for each set. This analysis is composed of two parts: one for examining the ratio of the undetected and late-detected well-clear violations and the other for investigating the ability to detect the threats, which would generate the upcoming violations, at a given time prior to the violations. An undetected violation means that a violation occurs outside the surveillance volume. A late-detected violation means that the first violation is incurred outside the surveillance volume but the threat enters the volume later. The ratio of both undetected and late-detected violations to the total well-clear violations was presented. To examine the ability of detecting the threats at given times before the well-clear violations, the time remaining to the violations when the threats first appeared in the surveillance volume was measured and analyzed. This interval would be potential time for preventive activity to avoid the violations. Average time and cumulative distribution for the time are presented.

C. Simulation environment and traffic scenario

The Airspace Concept Evaluation System (ACES) fast-time simulation tool was used to simulate NAS-wide operations of UAS and VFR flights. ACES can run a gate-to-gate simulation of air traffic at local, regional and national levels.⁹ It simulates flight trajectories using aircraft models derived from the Base of Aircraft Data (BADA)¹⁰ and traffic data consisting of departure times and flight plans obtained from recorded Airline Situation Display to Industry (ASDI) files and recorded radar data.

To investigate the encounters between UAS flights and VFR flights in Class E airspace, a traffic scenario of 45,026 flights was used in the ACES simulation. It involves nine different types of UAS missions, including wildfire monitoring, air quality monitoring, flood inundation and stream monitoring, air taxi transport, cargo delivery, and atmospheric sampling missions.¹¹ These missions constitute a total of 18,256 simulated UAS flights over the course of a single day. Each mission uses different types of UAS models such as RQ7A, MQ9A, RQ4, and C510. The partial mission profiles are shown in Fig. 2. The traffic scenario also contains 26,770 cooperative VFR flights in Class E airspace for a 24-hour period on Wednesday, July 25, 2012, which were generated from the 84th Radar Evaluation Squadron (RADES) data. The altitude distributions for both UAS and VFR flights are depicted in Fig. 3. In this ACES simulation, no UAS or VFR flights are maneuvered to avoid any ATC separation standards or potential well-clear violations.

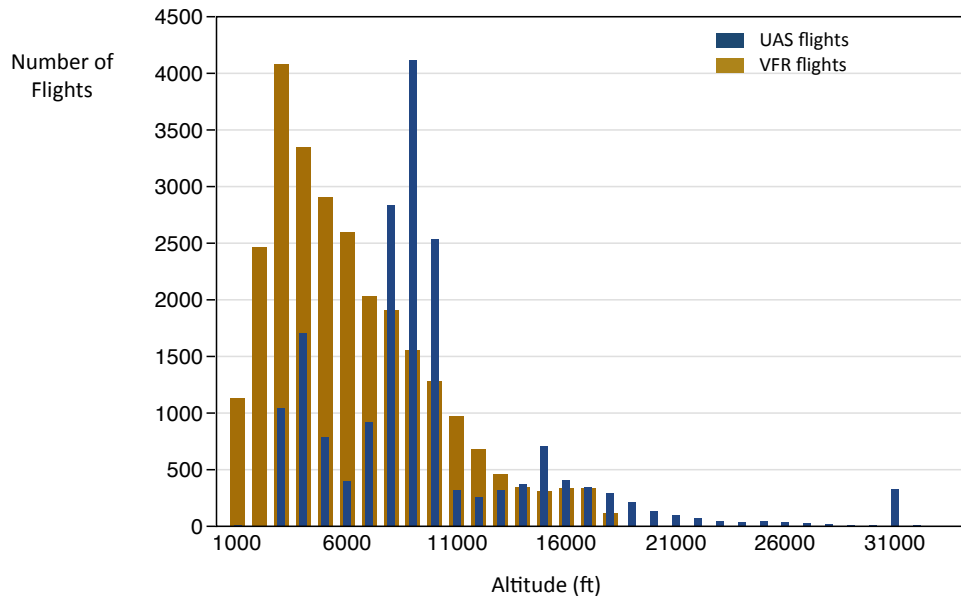


Figure 3. Max altitude distribution for UAS and VFR flights in the air traffic scenario

IV. Overall Analysis of Well-Clear Violations and Surveillance Parameters

The required surveillance parameters are closely related to the geometric characteristics of threats' positions when violations occurred. A surveillance system will be required to have sufficient range such that the DAA system has enough look-ahead time before a well-clear violation to avoid it. Therefore, this study investigated not only the geometric distributions of threats at the time when the violations occurred but also the geometric distributions of threats at 40, 80, and 120 seconds before the violations occurred.

A. Geometric relations between UAS flights and intruders

Figure 4 shows horizontal relative positions of threats at various time horizons prior to causing a well-clear violation. In Fig. 4 through Fig.7, the UAS flight is located at the origin with the velocity vector oriented right. When the violation occurred, all threats are located within horizontal 5 nmi range, but the maximum horizontal range of overtaking threats was less than 2 nmi. Fig. 4 also shows their relative positions 40, 80, and 120 seconds before the violations. As time to well-clear violation increases, the radius of the circular-

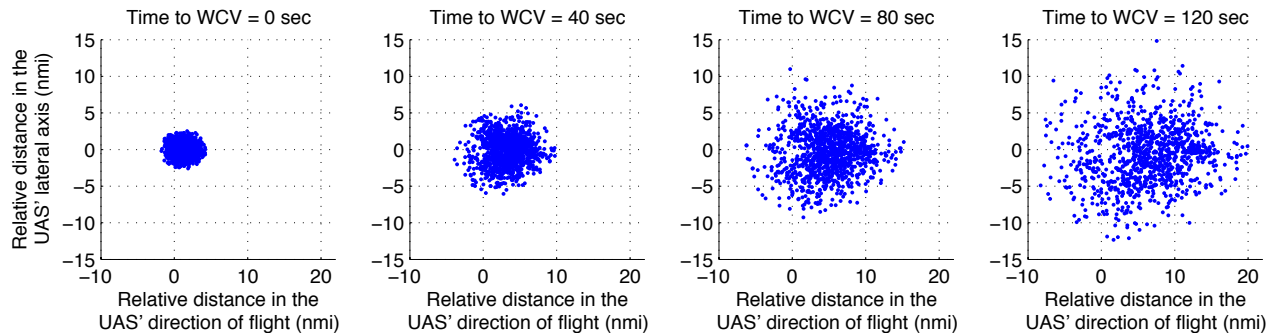


Figure 4. Horizontal relative positions of threats at the different times (0, 40, 80 and 120 sec) to well-clear violation (WCV). The UAS flight is located at the origin with the velocity vector oriented right.

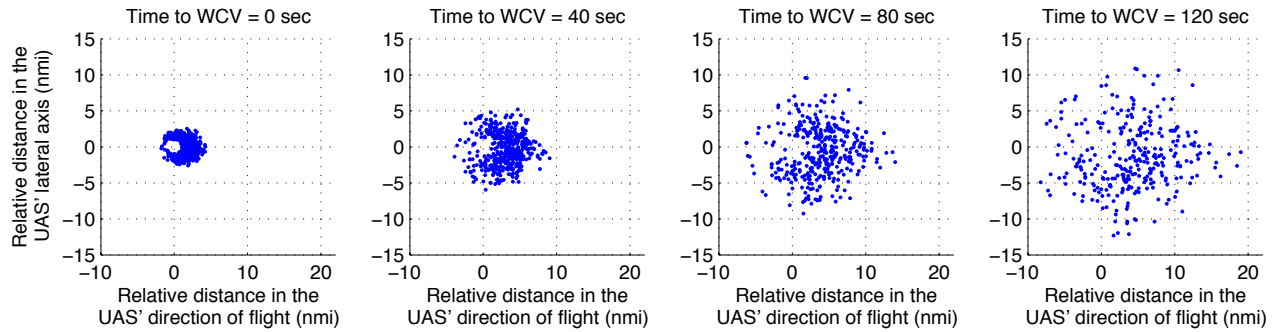


Figure 5. Horizontal relative positions of threats at the different times (0, 40, 80 and 120 sec) to well-clear violation (WCV). These plots show only the threats whose altitudes are within 400 ft of conflicting UAS. The UAS flight is located at the origin with the velocity vector oriented right.

shaped distribution of threats increases. Since Fig. 4 includes all threats including those above or below UAS flights, there are threats even within the horizontal distance threshold around the origin, which represents the *DMOD* value described in Section III-A. On the other hand, Fig. 5 shows that threats are outside of the horizontal distance threshold, *DMOD*, when well-clear violations occur since this figure contains only the threats within 400 ft of altitude difference. As expected, most threats were located ahead of the UAS flight.

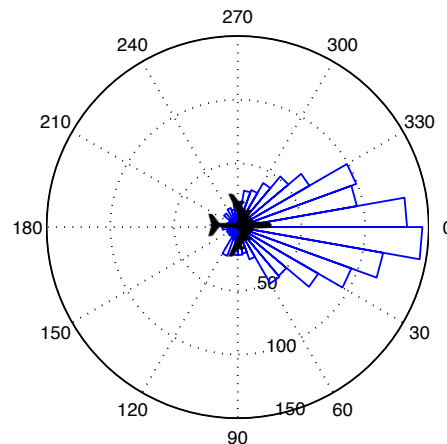


Figure 6. Angular distribution of intruders when they incurred the well-clear violations. The numbers in the outer circle denote the relative horizontal angles of threats in degrees and the size of the triangular bar indicates the number of flights. The number for each concentric circle (50, 100 and 150) refers to the number of flights.

Figure 6 gives detailed information on angular distribution of threats. The well-clear violations incurred within $\pm 30^\circ$ horizontally from the direction of flight is 50.8% of total violations, and those within $\pm 60^\circ$ constitute 75.2%.

Figure 7 shows the vertical distribution of threats in addition to the distribution in the longitudinal axis. Although most well-clear violations occurred within ± 475 ft, which is the altitude threshold for definition of well-clear violation, a number of violations occurred between 2,000 ft below and 1,000 ft below the UAS. As shown in Fig. 7, more well-clear violations with VFR flights occurs below the UAS than above the UAS, which means that the UAS may violate well-clear more often with climbing VFR flights rather than with descending VFR flights.

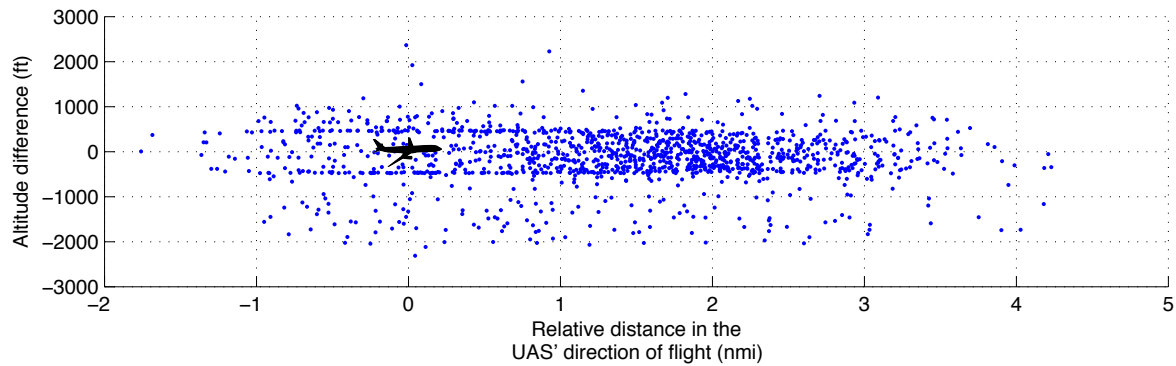


Figure 7. Horizontal and vertical distribution of intruders when they incurred well-clear violations.

B. Cumulative distribution for distances and angles to intruders

Figure 8 depicts the cumulative distribution function of horizontal distance to the threats. The maximum distance to threats is approximately proportional to the time to well-clear violation. When the violations occurred, all threats were located within 4.26 nmi. When the times to the violations are 40, 80 and 120 sec, all intruders were located within 9.78 nmi, 15.20 nmi, and 19.93 nmi, respectively. These results suggest that if DAA system designers specify 2 minutes as the required time for preventive actions, 20 nmi would be a sufficient range requirement for the surveillance system, although the performance also depends on algorithms and methods. Figure 8 also presents how many threats would be captured at a given time prior to well-clear violation by a surveillance system with a given range. For example, if the range of a surveillance system is 10 nmi, the system could be expected to detect all well-clear violations and the threats 40 sec in advance, but it could be expected to detect only 90% of the threats 80 sec in advance and only 70% of threats 2 minutes in advance.

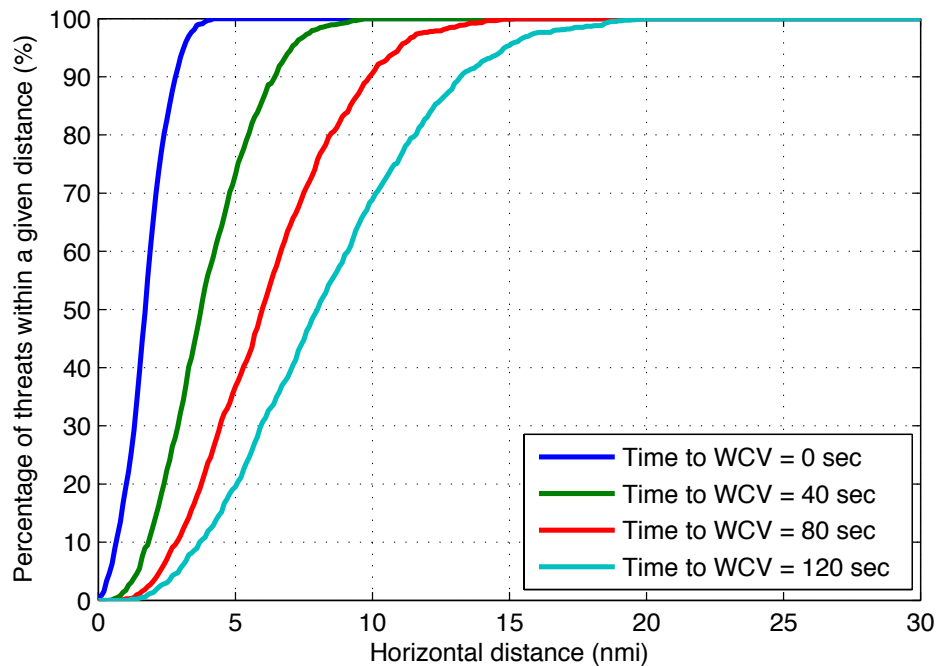


Figure 8. Cumulative distribution function of horizontal distance between threats and UAS flights.

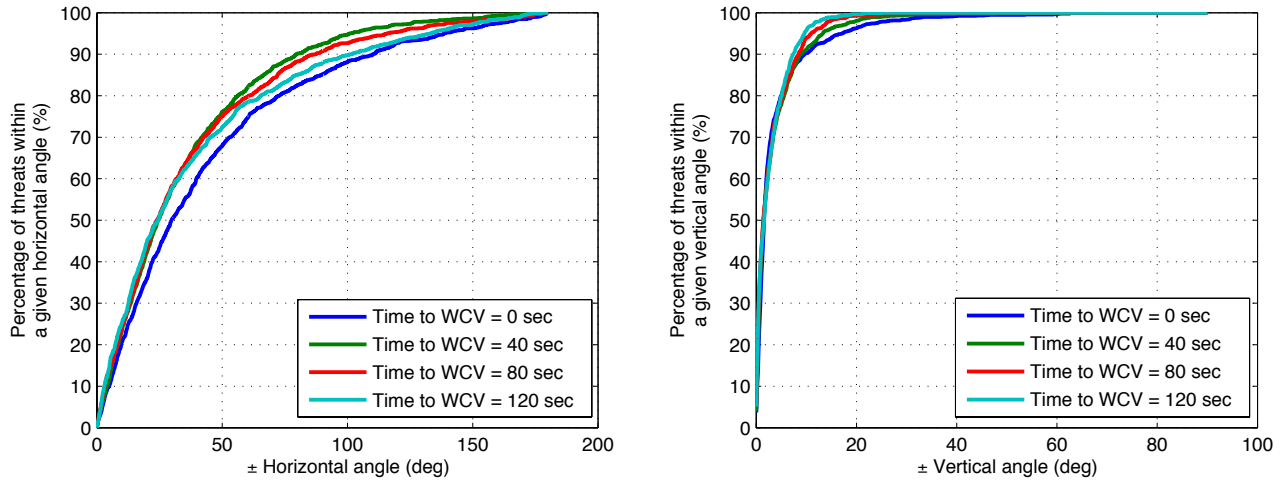


Figure 9. Cumulative distribution functions of horizontal and vertical angles of threats from UAS flights.

Figure 9 shows the cumulative distribution functions of horizontal and vertical angles to the threats. More than 90% of threats were located within $\pm 120^\circ$ horizontally at the time of well-clear violations and even at 120 sec before the violations, which means $\pm 120^\circ$ of horizontal field of regard (hFOR) is required to detect actual well-clear violations. More than 90% of intruders were located within $\pm 15^\circ$ vertically at all times, which means if a UAS is equipped with a sensor system with at least $\pm 15^\circ$ of vertical field of regard (vFOR), then more than 90% of threats can be detected even 120 sec before the violation.

V. Analysis for Different Sets of Surveillance Parameters

Based on the geometric analysis of well-clear violations in Section IV, discrete values for surveillance parameters were chosen to test different specific surveillance volumes. Three candidate ranges were selected; four horizontal and two vertical fields of regard were chosen. These parameter sets generate a total of 24 ($3 \times 4 \times 2$) surveillance volumes. Table 1 presents those parameter values.

Table 1. Surveillance parameters and their values to be used. Total 24 combinations were investigated.

Surveillance Parameters	Values
Surveillance Range	6, 10, and 20 nmi
Horizontal Field of Regard	$\pm 60, 90, 120,$ and 180°
Vertical Field of Regard	± 20 and 40°

A. Undetected and late-detected well-clear violations

Figure 10 shows the ratio of undetected well-clear violations to the total well-clear violations as a function of different surveillance volumes. The ratio did not vary for three different ranges: 6, 10, and 20 nmi. This was an expected result because all violations occurred within 5 nmi from the UAS flight as depicted in Fig. 8. Also, there was a little difference between the two vertical fields of regard: 20° and 40° . However, the ratio decreases as hFOR becomes wider. If a surveillance system is required to detect more than 90% of violations correctly, the hFOR of the system should be set to 120° or larger. This figure also shows the ratio of well-clear violations that were detected late. The ratio of late-detected violations generally decreases as hFOR increases; however, it is higher for 180° of hFOR. Although most undetected violations for 120° of hFOR might be successfully detected with 180° of hFOR, many of them were detected late. Future research should investigate the late-detected well-clear violations further.

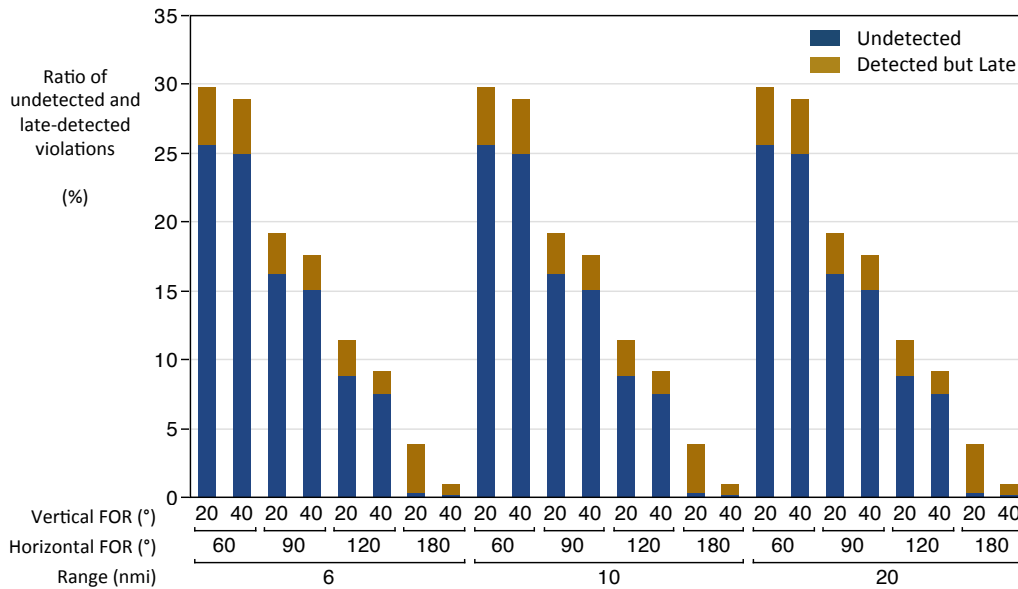


Figure 10. Ratio of undetected and late-detected well-clear violations to the total number of well-clear violations.

For one surveillance volume with 10 nmi of range, 120° of hFOR and 20° of vFOR, the characteristics of undetected violations was investigated. Figure 11 shows the cumulative distribution functions of horizontal distances and vertical angles to the positions where the undetected violations occurred. All violations occurred within 2 nmi of horizontal distance and 65° of vFOR. This result suggests that most undetected violations could be detected if a UAS flight were equipped with a secondary sensor that had short range (around 2 nmi) but wide vertical field of regard (around 65°) to cover the horizontal angles the primary sensor does not cover.

An interesting observation is that approximately 80% of intruders among 120 intruders that caused undetected well-clear violations appeared within the surveillance volume at least once although they did not prompt a well-clear violation during the period they stayed inside the volume. This means that approximately 20% of the intruders related to undetected violations never entered within the given surveillance volume with 10 nmi of range, 120° of hFOR and 20° of vFOR. Such an event may occur when either the UAS flight or the intruder does not fly in a straight line. An intruder tracking algorithm could be improved to detect such violations by considering flights that do not fly in a straight line.

B. Detected well-clear violations

Figure 12 presents the average time to well-clear violation when threats first appear in the surveillance volume for the intruding event that caused violations. The average time to violation increases as the range and horizontal field of regard increase. If 10 nmi of range, 120° of hFOR and 20° of vFOR are chosen as surveillance parameters, the average time to violation is 147.5 sec. Even though the average time represents a general trend of threats, the average values may not be appropriate for selecting a reasonable set of surveillance parameters because it cannot represent all violations when its variance is large. Therefore, the cumulative distribution function of the time to well-clear violation is used to determine reasonable sets of surveillance parameters.

Figure 13 shows those cumulative distribution functions for different sets of surveillance parameters. Although the distributions for two vFOR, 20° and 40°, were not identical, their shapes were similar. Therefore, Fig. 13 has the plots for 20° of vFOR only. When only 20 sec are left until the well-clear violation, all twelve sets of surveillance parameters have similar performance, that is, more than 90% of upcoming violations could be detected. However, as the time to violation increases, the percentage of detected threats rapidly decreases for a surveillance system with 6 nmi of range. When the range is 10 nmi, the percentage

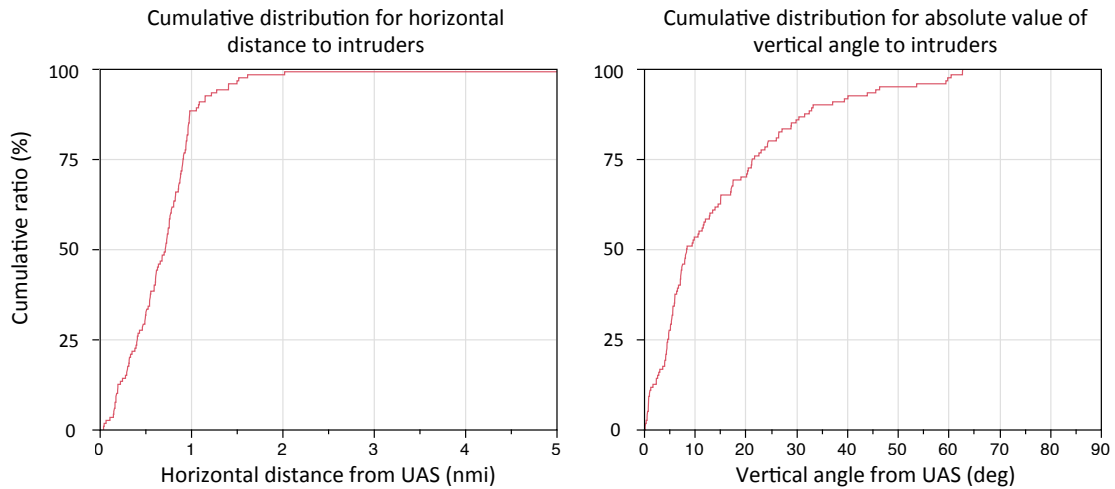


Figure 11. Cumulative distribution functions of horizontal distance and vertical angle to threats when well-clear violations occurred outside the surveillance volume. The distributions are the results for a set of 10 nmi of range, 120° of hFOR, and 20° of vFOR.

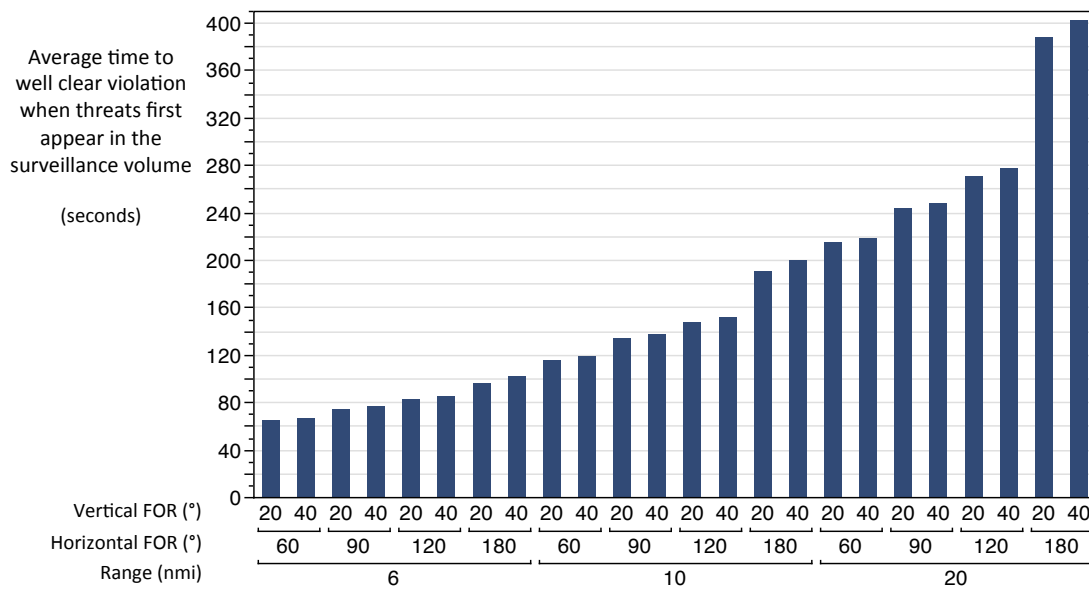


Figure 12. Average time to well-clear violation when intruders first appear in the surveillance volume.

is gradually decreasing as the time to violation increases up to 60 sec. Then, for larger than 60 sec, it is rapidly decreasing. For a surveillance system with 20 nmi of range, the percentage decreases more gradually as the time to violation increases up to 120 sec. It is noticed that the time to the well-clear violation is more sensitive to the surveillance range than hFOR.

Figure 13 can be applied to surveillance system design. For example, if the goal is to detect more than 90% of intruders related to upcoming well-clear violations 40 sec before, seven out of twelve sets are plausible. So, in this case, a set of 10 nmi of range, 120° of hFOR and 20° of vFOR is enough. However, if the goal is to detect the threats that cause a well-clear violation 80 sec in advance, only three sets are available. In this case, range should be at least 20 nmi and hFOR should be at least 90° . Table 2 presents plausible sets of surveillance parameters for desired time before the violations.

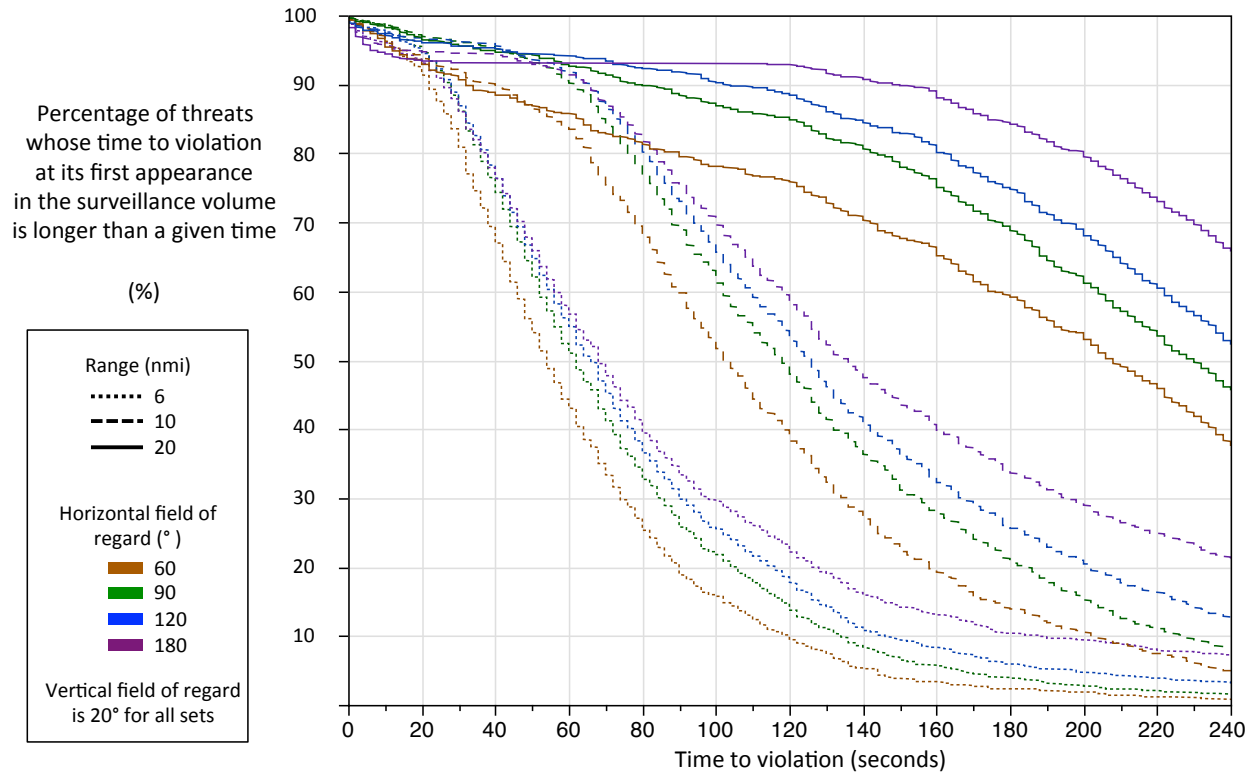


Figure 13. Ratio of threats whose time to well-clear violation at their first appearance in the surveillance volume is longer than a given time.

Table 2. Sets of surveillance parameters that could be used to detect more than 90% of upcoming well-clear violations at given desired time before the violations. Based on the results in Fig. 13, these sets were derived from 12 surveillance volumes with 20° of vFOR.

Desired look-ahead time before the violations	Plausible sets of surveillance parameters {range (nmi), hFOR (°), vFOR (°)}
40 sec	{10, 60, 20}, {10, 90, 20}, {10, 120, 20}, {10, 180, 20}, {20, 90, 20}, {20, 120, 20}, {20, 180, 20}
60 sec	{10, 90, 20}, {10, 120, 20}, {10, 180, 20}, {20, 90, 20}, {20, 120, 20}, {20, 180, 20}
80 sec	{20, 90, 20}, {20, 120, 20}, {20, 180, 20}
100 sec	{20, 120, 20}, {20, 180, 20}
120 sec	{20, 180, 20}

VI. Concluding Remarks and Directions for Future Research

This paper analyzed the characteristics of a particular type of encounter, specifically well-clear violations, between UAS flights and cooperative VFR flights. A fast-time simulation tool, ACES, was used to generate a database of well-clear violations using an air traffic scenario that contains representative UAS missions and NAS-wide cooperative VFR traffic for a single day. The characteristics of these encounters and the circumstances leading up to the violations were logged and parsed in a way that will allow DAA surveillance system designers to select the required range and fields of regard of the system's sensors to meet overall

system safety metrics. Examples of such metrics are the time to violation at which threats are detected and the percentages of threat aircraft that are never detected or detected late.

Examples of the requirements that may be derived from the simulation results are presented in this paper, but the specific form of the data necessary to meet safety requirements will depend upon the requirements being developed by RTCA's Special Committee 228. One key result is that all well-clear violations in this study occurred at a range under 5 nmi from the UAS and more than 75% of them occur within horizontal $\pm 60^\circ$ from the direction of UAS heading. Based on this general analysis of aircraft encounters, 24 sets of candidate surveillance system volumes were selected to evaluate safety metrics as a function of the surveillance volume. The ratio of undetected and late-detected encounters to the total encounters was most sensitive to the horizontal field of regard. When horizontal field of regard was larger than 120° , more than 90% of encounters were detected before they became well-clear violations. The time to violation at which a threat was first detected was most sensitive to surveillance range, as expected. The horizontal and vertical field of regard did not have a substantial effect on the available alerting time. As an example, if the safety metrics dictate that the DAA system must detect at least 90% of threats at least 60 sec before violation, then the surveillance system should have a 10 nmi surveillance range and at least $\pm 90^\circ$ of horizontal field of regard and $\pm 20^\circ$ of vertical field of regard. If, instead, more than 90% of threats are required to be detected 80 sec before violation, then the required surveillance range should be larger than 20 nmi. The database for encounters collected from this simulation study will be useful for surveillance system designers to make tradeoffs between these parameter values to suit their UAS' capabilities.

Although this study provided significant information on DAA surveillance performance tradeoff requirements, there is still ample room for further research. In this study, the database of well-clear violations was built with a single day operations of UAS and cooperative VFR traffic. A sensitivity analysis with different density of the traffic and various types of UAS missions with different flight characteristics might be required to evaluate how encounter characteristics and the performance of surveillance system are affected by those parameters for a future study. This study also investigated unmitigated encounters with no active separation system employed; additional requirements will be derived from studies of preventive maneuvers to avoid violations. The results for different days' background traffic with different UAS missions and performance parameters will be explored to analyze the sensitivity of the requirements to the parameters. This study examined three characteristics of surveillance systems, which are range, horizontal field of regard, and vertical field of regard, with a fixed sensor scan rate, 2 sec. Different sensor scan rates should be studied in future research to investigate its effects on detecting well-clear violations. Finally, additional definitions of the well-clear separation standard should be evaluated to inform an appropriate selection of that standard.

Acknowledgments

The authors would like to thank Mr. Confesor Santiago, Dr. Marcus Johnson, and Dr. Ki Hwan Lee for discussions on preparing experimental plans. Thanks are also due to Dr. Todd Lauderdale, Dr. Min Xue, Mr. Todd Farley, and Ms. Katharine Lee for their thoughtful reviews and suggestions for improving the paper.

References

- ¹Federal Aviation Administration (FAA), *Sense and Avoid (SAA) for Unmanned Aircraft Systems (UAS) : Second Caucus Workshop Report*, January 2013.
- ²Federal Aviation Administration (FAA), *Integration of Unmanned Aircraft Systems into the National Airspace System: Concept of Operations V2.0*, September 2012.
- ³Maki, E., Weinert, A., and Kochenderfer, M., "Efficiently Estimating Ambient Near Mid-Air Collision Risk for Unmanned Aircraft," *Proceedings of the 10th AIAA Aviation Technology, Integration, and Operations (ATIO) Conference*, AIAA, Fort Worth, Texas, September 2010.
- ⁴Kochenderfer, M. J., Kuchar, J. K., Espindle, L. P., and Griffith, J. D., "Uncorrelated Encounter Model of the National Airspace System Version 1.0," Project Report ATC-345, Massachusetts Institute of Technology, Lincoln Laboratory, November 2008.
- ⁵Weibel, R., Edwards, M., and Fernandes, C., "Establishing a Risk-Based Separation Standard for Unmanned Aircraft Self Separation," *Proceedings of the 11th AIAA Aviation Technology, Integration, and Operations (ATIO) Conference*, AIAA, Virginia Beach, Virginia, September 2011.
- ⁶Lee, S. M., Park, C., Johnson, M. A., and Mueller, E. R., "Investigating Effects of "Well Clear" Definitions on UAS Sense-And-Avoid Operations," *Proceedings of the 13th AIAA Aviation Technology, Integration, and Operations (ATIO) Conference*, AIAA, Los Angeles, California, August 2013.

⁷Hottman, S. and Hansen, K., *Literature Review on Detect, Sense, and Avoid Technology for Unmanned Aircraft Systems*, Federal Aviation Administration William J. Hughes Technical Center, 2009.

⁸Muñoz, C., Narkawicz, A., and Chamberlain, J., “A TCAS-II Resolution Advisory Detection Algorithm,” *Proceedings of AIAA Guidance, Navigation, and Control Conference*, AIAA, Boston, Massachusetts, August 2013.

⁹George, S. E., Satapathy, G., Manikonda, V., Wieland, F., Refai, M. S., and Dupee, R., “Build 8 of the Airspace Concept Evaluation System,” *Proceedings of the AIAA Modeling and Simulation Technologies (MST) Conference*, AIAA, Portland, Oregon, August 2011.

¹⁰Nuic, A., Poles, D., and Mouillet, V., “BADA: An advanced aircraft performance model for present and future ATM systems,” *International Journal of Adaptive Control and Signal Processing*, Vol. 24, No. 10, 2010, pp. 850–866.

¹¹Ayyalasomayajula, S., Wieland, F., Trani, A., and Hinze, N., “Unmanned Aircraft System Demand Generation and Airspace Performance Impact Prediction,” *Proceedings of the 32nd IEEE Digital Avionics Systems Conference*, IEEE, Syracuse, NY, October 2013.